hydrogen

MDPI

Article

Pinch-Guided Heat Integration for Hydrogen Production from Mixed Plastic Waste

Fiyinfoluwa Joan Medaiyese, Maryam Nasiri Ghiri, Hamid Reza Nasriani *, Leila Khajenoori and Khalid Khan

School of Engineering & Computing, University of Lancashire, Preston PR1 2HE, UK; fjmedaiyese@lancashire.ac.uk (F.J.M.); mnasiri-ghiri@lancashire.ac.uk (M.N.G.); lkhajenoori@lancashire.ac.uk (L.K.); kkhan5@lancashire.ac.uk (K.K.)

* Correspondence: hrnasriani@lancashire.ac.uk

Abstract

The conversion of plastic waste into hydrogen offers a promising waste-to-value pathway, but its industrial viability is constrained by high external energy demand associated with thermochemical processing. This study evaluates the energy performance of hydrogen production from mixed plastic waste via pyrolysis and in-line steam reforming, with a focus on reducing utility consumption through systematic heat integration. A steady-state process model was developed in Aspen Plus for a representative mixture of polyethylene, polypropylene, and polystyrene, followed by detailed energy analysis and pinch-based heat integration using Aspen Energy Analyser. Baseline utility requirements were quantified and compared against optimised configurations incorporating targeted heat exchanger network modifications. The base-case analysis identified significant recoverable heat, enabling a reduction in total external utilities from 7.14 to 2.88 GJ h^{-1}, corresponding to a 59.6% decrease in utility demand. Sequential heat integration scenarios further reduced heating and cooling duties while maintaining process operability, demonstrating the effectiveness of iterative, pinch-guided design. The results show that high-temperature waste-plastic-to-hydrogen systems need not be utility-dominated when energy integration is embedded at the design stage. These findings highlight heat integration as a critical enabler for improving the energy efficiency and sustainability of pyrolysis–reforming routes and provide a robust framework for developing scalable, low-carbon hydrogen production from plastic waste.

Keywords: hydrogen production; plastic waste valorisation; waste-to-hydrogen; heat integration; pinch analysis; aspen energy analyser; heat exchanger network

Academic Editor: Zhang-Hui Lu

Received: 29 December 2025
Revised: 12 February 2026
Accepted: 25 February 2026
Published: 4 March 2026

1. Introduction

The continued reliance on fossil fuels has led to increased carbon dioxide (CO_2) emissions, contributing to global warming, air pollution, and resource depletion [1,2]. Transitioning to clean and sustainable energy carriers, such as hydrogen, is therefore critical for reducing environmental impacts and meeting future energy demands [3,4]. Hydrogen offers the advantage of zero carbon emissions at the point of use, only producing water vapour after combustion and can be produced from a variety of renewable and waste-derived feedstocks, making it a promising alternative to conventional fossil fuels [5]. Hydrogen production can be achieved from multiple feedstocks, including water, natural gas, and conventional fossil fuels. To promote sustainability, research is increasingly focusing on alternative sources, including renewable biomass and plastic waste [6,7].

Global energy systems remain dominated by fossil-based resources, which have underpinned industrial development and economic growth for decades but continue to impose significant environmental and climatic burdens [8–11]. Conventional energy sources, particularly coal, oil, and natural gas, are associated with substantial carbon dioxide emissions across their extraction, processing, and utilisation stages [12]. In response to growing demand and declining conventional reserves, unconventional energy resources have assumed an increasingly prominent role in the global energy mix. These resources, while enhancing energy security and supply resilience, are often characterised by higher energy intensity, greater process complexity, and elevated lifecycle emissions if not managed efficiently [13–15]. As a result, the exploitation and processing of unconventional energy sources have intensified concerns regarding greenhouse gas emissions, climate change, and the long-term sustainability of carbon-intensive energy pathways [16–18].

Against this backdrop, the energy transition has emerged as a central objective for achieving climate mitigation targets, emphasising efficiency improvements, decarbonisation, and the integration of low-carbon and circular solutions [19–23]. Sustainable energy systems increasingly prioritise not only alternative energy carriers, such as hydrogen, but also the optimisation of existing and emerging processes to minimise energy losses and environmental impacts [24–28]. In parallel, effective waste management has become a critical component of sustainable development, particularly as waste streams grow in volume and complexity [18,29–33]. Converting waste materials into valuable energy products offers a dual opportunity to reduce environmental pollution while displacing primary fossil energy consumption. When coupled with systematic energy integration and efficiency-driven design, waste-to-energy pathways can contribute meaningfully to emissions reduction, resource conservation, and the broader transition towards resilient, low-carbon energy systems [33–40].

Global plastic production has increased dramatically over recent decades due to the widespread use of plastics in industries such as electronics, transportation, construction, healthcare, and packaging, driven by their lightweight, durability, versatility, and low production cost [6,7,41–47]. As a result, plastic production rose from 1.5 million tonnes in 1950 to over 400 million tonnes in 2022, with packaging accounting for the largest share of total plastic use [48–54]. The continuous growth in plastic consumption has led to a significant accumulation of non-biodegradable plastic waste, posing serious environmental risks. Improper disposal has resulted in substantial plastic leakage into marine ecosystems, with an estimated 4–12 Mt/year entering the oceans, adversely affecting ecosystems and human health [55,56].

Plastic waste, as an abundant and underutilised resource, can be converted into hydrogen through thermochemical processes, providing a “waste-to-value” pathway aligned with circular economy principles [57,58].

Hydrogen can be produced through a range of established and emerging technologies, including water electrolysis, photocatalytic water splitting, and biomass conversion. Water electrolysis is a mature and efficient pathway when coupled with low-carbon electricity and plays a central role in many decarbonisation strategies; however, it is primarily electricity-driven. Photocatalytic water splitting remains under active development, with current solar-to-hydrogen efficiencies typically below 10%. Biomass-based hydrogen production is constrained by feedstock variability, complex composition, and purification requirements, which influence scalability and process integration [59].

Thermochemical conversion of waste plastics via pyrolysis with in-line reforming represents a complementary pathway that simultaneously addresses waste management and hydrogen production. Although this route operates at high temperatures, it provides significant opportunities for internal heat recovery and process integration, making it

particularly suitable for system-level energy analysis and optimisation, which is the focus of the present study.

Among thermochemical options, hydrogen can be produced from waste plastics primarily via single-stage gasification or through pyrolysis combined with in-line reforming [33,57,59]. While single-stage gasification is simpler, it suffers from tar formation and relatively low hydrogen yields, typically below 20 wt%. In contrast, pyrolysis–reforming achieves higher hydrogen yields (>30 wt%), operates at lower temperatures, and produces a tar-free syngas stream, with performance varying depending on plastic type [60,61]. Consequently, hydrogen production routes that valorise waste streams and reduce reliance on primary resources have gained increasing attention.

Among the thermochemical approaches, pyrolysis combined with in-line reforming has gained attention due to its ability to convert hydrocarbon-rich feedstocks into hydrogen-rich syngas while minimising tar formation. Various reforming strategies can be employed, including steam reforming, partial oxidation, dry reforming, and tri-reforming. Steam reforming is widely used industrially for its simplicity and high thermal efficiency (up to 85%) [62,63], while dry reforming can utilise CO_2 as a reactant, though it is limited by the reverse water–gas shift reaction [64,65]. Tri-reforming, combining steam, CO_2, and oxygen, is still at an early stage of development [66].

The hydrogen yield from pyrolysis–reforming processes depends critically on operating parameters, particularly the reforming temperature and the steam-to-plastic ratio. Higher reforming temperatures accelerate reaction rates and increase the extent of endothermic steam reforming reactions, while optimal steam-to-plastic ratios enhance hydrogen production by promoting both the reforming and water–gas shift reactions [67–73]. However, excessively high steam levels increase energy requirements for steam generation, risk catalyst sintering, and raise downstream separation costs [61,62,74]. While plastic pyrolysis–reforming is a promising pathway for hydrogen production, it remains energy intensive [59] and has received limited attention regarding process-wide thermal efficiency and heat integration. This study addresses this by quantifying energy demands and identifying opportunities to reduce process energy intensity, providing a framework for more sustainable hydrogen production from mixed plastic waste.

Energy analysis, including pinch analysis and heat integration for the process, plays a crucial role in identifying process inefficiencies and enabling optimisation strategies that reduce both energy consumption and operating costs [72,73]. In industrial hydrogen production, energy-intensive steps such as reforming, water–gas shift reactions, and gas purification significantly influence overall process efficiency and economic viability [75]. Consequently, systematic energy analysis provides a robust framework for improving thermal performance and enhancing the sustainability of hydrogen production processes [76–86].

Recent papers on pyrolysis–reforming of plastic and biomass-derived feeds largely concentrates on optimising reaction conditions, catalysts and downstream separation to maximise hydrogen yield and purity, with far less emphasis on energy integration of the system [87,88]. Building on this body of work, the present study examines system-level energy performance by quantifying process-wide energy demands and applying pinch-analysis to identify minimum utility targets and heat integration potential. The study investigates hydrogen production from plastic waste via a pyrolysis and in-line reforming route, with particular emphasis on a mixed plastic feedstock comprising high-density polyethylene, polypropylene, and polystyrene. Previous studies have successfully applied pinch analysis to hydrogen production from waste glycerol, biogas, and biomass gasification systems [89–91], demonstrating substantial reductions in heating and cooling utility demands. However, the use of pinch analysis for hydrogen production from mixed plastic waste via pyrolysis with in-line reforming has received limited attention. To the author's

knowledge, this study represents the first system-level, pinch-based energy integration analysis of a mixed plastic pyrolysis–reforming hydrogen production process. The Aspen Plus tool is used to identify energy savings potential, while the Aspen Energy Analyser tool is used to perform energy analysis, including pinch analysis and heat integration for the process.

2. Methodology

2.1. Modelling and Simulation of the Process

The hydrogen production process from mixed plastic waste was modelled using Aspen Plus V14. The process considers a blend of high-density polyethylene (HDPE), polypropylene (PP), and polystyrene (PS) in an equal mass ratio (1:1:1), corresponding to a total feed rate of 300 kg/h. HDPE, PP, and PS were selected as representative plastic materials due to their high carbon and hydrogen contents and favourable behaviour during pyrolysis [57,74]. Unlike PET, which contains oxygenated functional groups that reduce fuel quality and hydrogen yield while promoting catalyst deactivation [92], polyolefin plastics produce hydrocarbon-rich pyrolysis products suitable for reforming. Consequently, PET was excluded from this study. The corresponding value of weight-average molecular weight (Mw), number-average molecular weight (Mn), and polydispersity index (PDI) of a polymer is presented in the last author's published paper [93]. These parameters are essential as they indicate the size of the polymer molecules and the uniformity of their distribution, which are key factors in determining the physical, mechanical and processing properties of the polymer. Detailed analytical characterisation of pyrolysis products is available in our previous work [93], which informed the kinetic parameters and product distributions used in this study.

The POLYSL (Sanchez-Lacombe) property method was employed for the pyrolysis stage due to its suitability for polymer systems and thermal degradation processes. The simulation is based on the following assumptions. The char is assumed to consist solely of plastic residues, while the gaseous products are composed of light hydrocarbons, including methane, ethane, ethylene, propane, propylene, butane, and butylene. All simulations were performed under steady-state and isothermal conditions, with the plastics undergoing slow pyrolysis at 500 °C and 1 bar. Figure 1a illustrates the overall process flowsheet for the pyrolysis–reforming system designed for this study. Polystyrene (PS), high-density polyethylene (HDPE), and polypropylene (PP), each with a mass flow rate of 100 kg/h at ambient conditions (25 °C, 1 bar), were fed into a mixer (MIXER) to form a single mixed plastics stream (MIXPLAST). This stream was then heated in a heater (HEATER) to 500 °C, the designated pyrolysis temperature, producing the heated plastics stream (HXPLAST). Given the slow pyrolysis conditions, the pyrolysis reactor was modelled using a batch reactor (RBatch module), incorporating detailed kinetic mechanisms that account for polymer degradation pathways such as random scission, hydrogen abstraction, β-scission, depolymerisation, and termination reactions. The RBatch was employed to incorporate batch-derived kinetic data within an otherwise continuous, steady-state process flowsheet, thereby reflecting the predominantly continuous nature of industrial pyrolysis operation [94,95]. In this context, the specified mass flow rate represents a steady-state equivalent throughput, enabling consistent integration with downstream reforming, heat recovery, and utility calculations [94]. This hybrid modelling approach, where batch-scale kinetic information is mapped onto nominal continuous operation, is frequently adopted when kinetic parameters are obtained from batch experiments but the objective is to evaluate whole process performance [95,96]. Kinetic parameters for HDPE, PP, and PS were adopted from literature sources [93,97–99] and implemented within Aspen Plus to represent realistic thermal cracking behaviour. The pyrolysis products were categorised into

light gases (C_1-C_4 hydrocarbons and hydrogen), condensable hydrocarbons, and solid char, with the gaseous fraction directed to downstream processing. Following pyrolysis, the solid char (CHAR) was removed from the volatile products (VOLATILE) via a separator (SEP). The volatile hydrocarbon stream was subsequently cooled (COL-VOL) to −5 °C before entering a flash separator (FLSHSEP1), enabling nearly complete separation of the gas and liquid phases. The reforming and subsequent water–gas shift (WGS) reactions were modelled using Gibbs free-energy minimisation reactors (RGibbs), assuming thermodynamic equilibrium. The application of RGibbs reactors is well established in system-level process simulation and energy integration studies, where the primary objective is to evaluate overall mass and energy balances rather than detailed reaction kinetics [100]. At high reforming temperatures, product distributions are strongly influenced by thermodynamic constraints. As a result, equilibrium-based modelling provides a reasonable first-order approximation for evaluating hydrogen yield trends and system-level energy-performance, despite potential kinetic limitations. Consequently, the predicted hydrogen production and associated heat duties represent idealised performance and should be interpreted as upper-bound estimates rather than exact predictions of industrial operation.

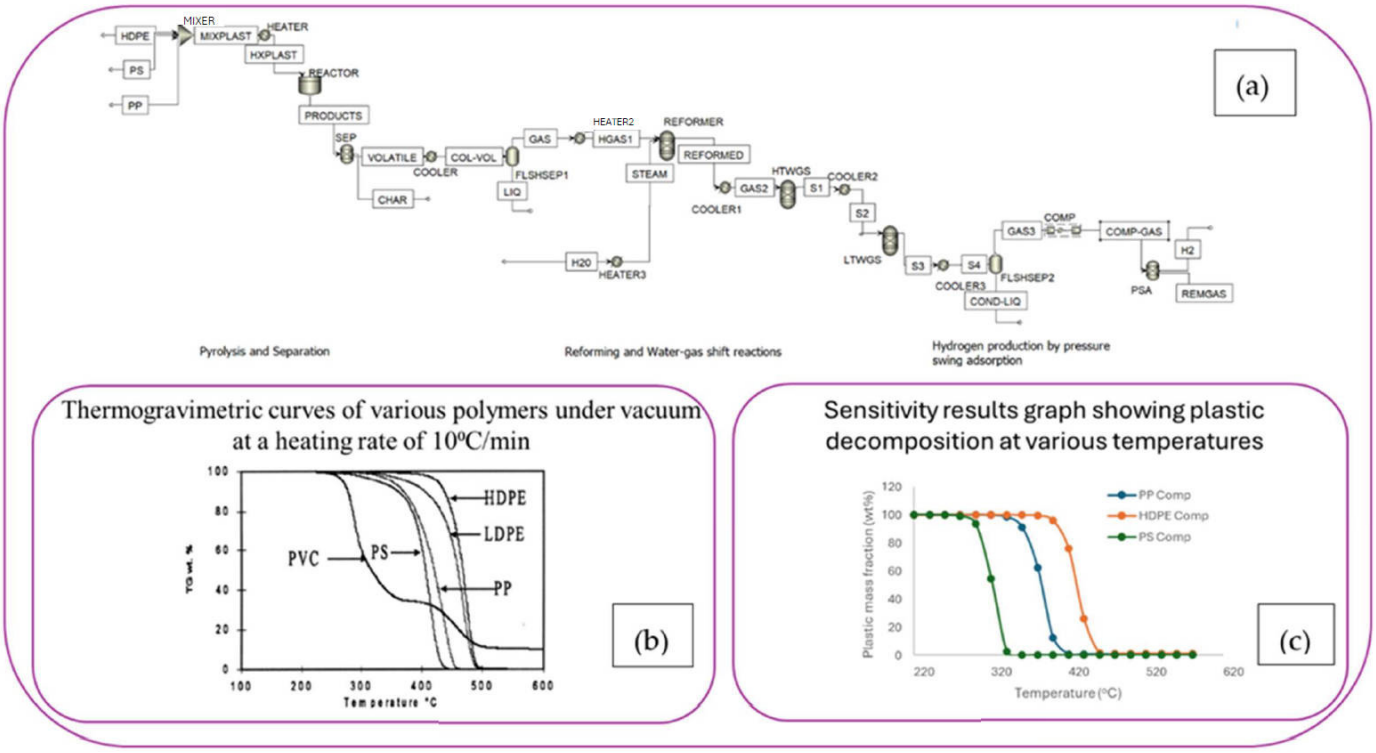

Figure 1. (**a**) Process flow diagram of the pyrolysis–reforming system. (**b**) Thermogravimetric curves of polymers obtained under vacuum at a heating rate of 10 °C min^{-1} [101]. (**c**) Sensitivity analysis showing order of thermal stability of plastic decomposition, validating the thermogravimetric behaviour observed in (**b**).

The gaseous hydrocarbons (GAS), primarily light hydrocarbons and hydrogen, were then heated (HGAS1) and sent to the steam reforming section, where steam is introduced at a 2:1 mass ratio relative to plastics, based on results from the author's previous study on optimal conditions for hydrogen production [93]. Steam reforming was conducted at 700 °C using steam as the reforming agent, while syngas upgrading was achieved through a two-stage WGS configuration comprising a high-temperature and a low-temperature reactor to maximise CO conversion to hydrogen. For the reforming and syngas processing sections, the property method was switched to Peng–Robinson Boston–Mathias (PR-BM), which is

well-suited for high-temperature gas-phase systems and syngas mixtures. Downstream of the WGS reactors, the product gas stream (S3) was cooled (S4) to 38 °C, slightly above ambient temperature, and sent to a flash separator (FLSHSEP2) to remove residual water (COND-LIQ). Hydrogen purification was subsequently simulated using a pressure swing adsorption (PSA) system, represented in Aspen Plus by a combination of compression and separation units to achieve hydrogen enrichment (H_2 separation from TAILGAS).

Model validation was performed through sensitivity analysis of plastic mass conversion with respect to temperature. The predicted thermal stability trends of HDPE, PP, and PS were consistent with reported thermogravimetric analysis data from literature, confirming the reliability of the simulation framework under slow pyrolysis conditions. A detailed description of the process model, reaction mechanisms, and validation results is provided in the authors' previous work [93]. Figure 1 shows the process flow diagram and the validation results of the process. Figure 1b presents representative thermogravimetric (TGA) curves for common packaging plastics, adapted from the work of Miranda et al. [101], which illustrate the relative thermal stability of HDPE, LDPE, PP, and PS. These curves are included to provide a qualitative comparison of polymer decomposition behaviour and to contextualize the modelling approach adopted in this study.

While the absolute decomposition temperatures reported by Miranda et al. [101] differ slightly from those obtained in the present work as shown in Figure 1c, this is attributed to differences in pyrolysis conditions, as their study considered moderate pyrolysis at higher heating rates, whereas the present simulation is based on slow pyrolysis conditions. Nevertheless, the relative order of polymer stability remains consistent.

2.2. Baseline Energy Assessment

Building upon the validated steady-state simulation of the pyrolysis–reforming process described in Section 2.1, a comprehensive energy analysis was initiated to quantify the thermal demands of the hydrogen production system. Using Aspen Plus, utilities (heating and cooling) were assigned to every unit operation requiring thermal regulation, including the batch pyrolysis reactor, the Gibbs reforming reactor, and all auxiliary heat exchangers and flash separators. The appropriate utilities required for the unit operations used in the flowsheet were defined as shown in Figure 2. These utilities were then allocated to the respective unit operations based on the specific temperature requirements, as depicted in Figure 3. This allocation ensures that the energy demands of each unit are correctly represented before proceeding to energy integration analysis.

All utilities were defined solely for thermal control and did not participate in chemical reactions, establishing a clear baseline of the external energy required to maintain the process at optimal operating conditions.

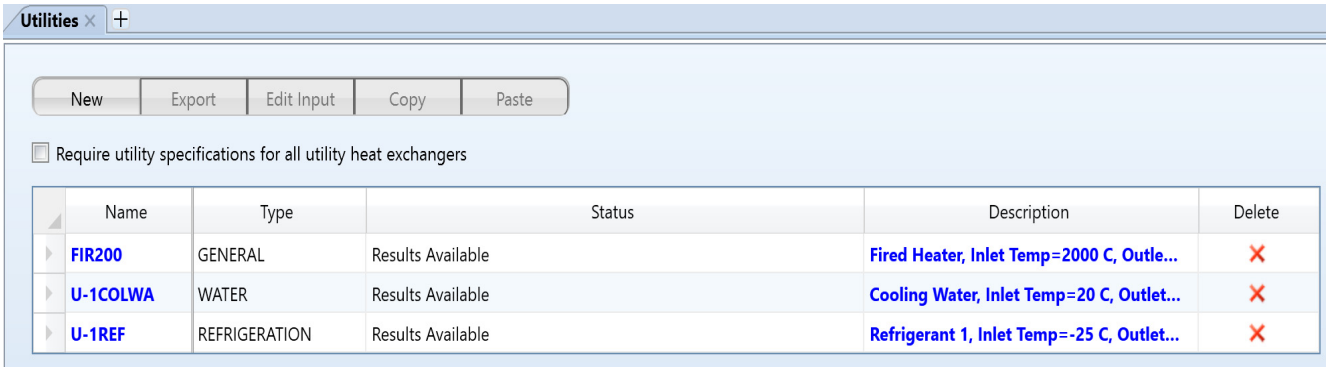

Figure 2. Required utilities applied for energy analysis.

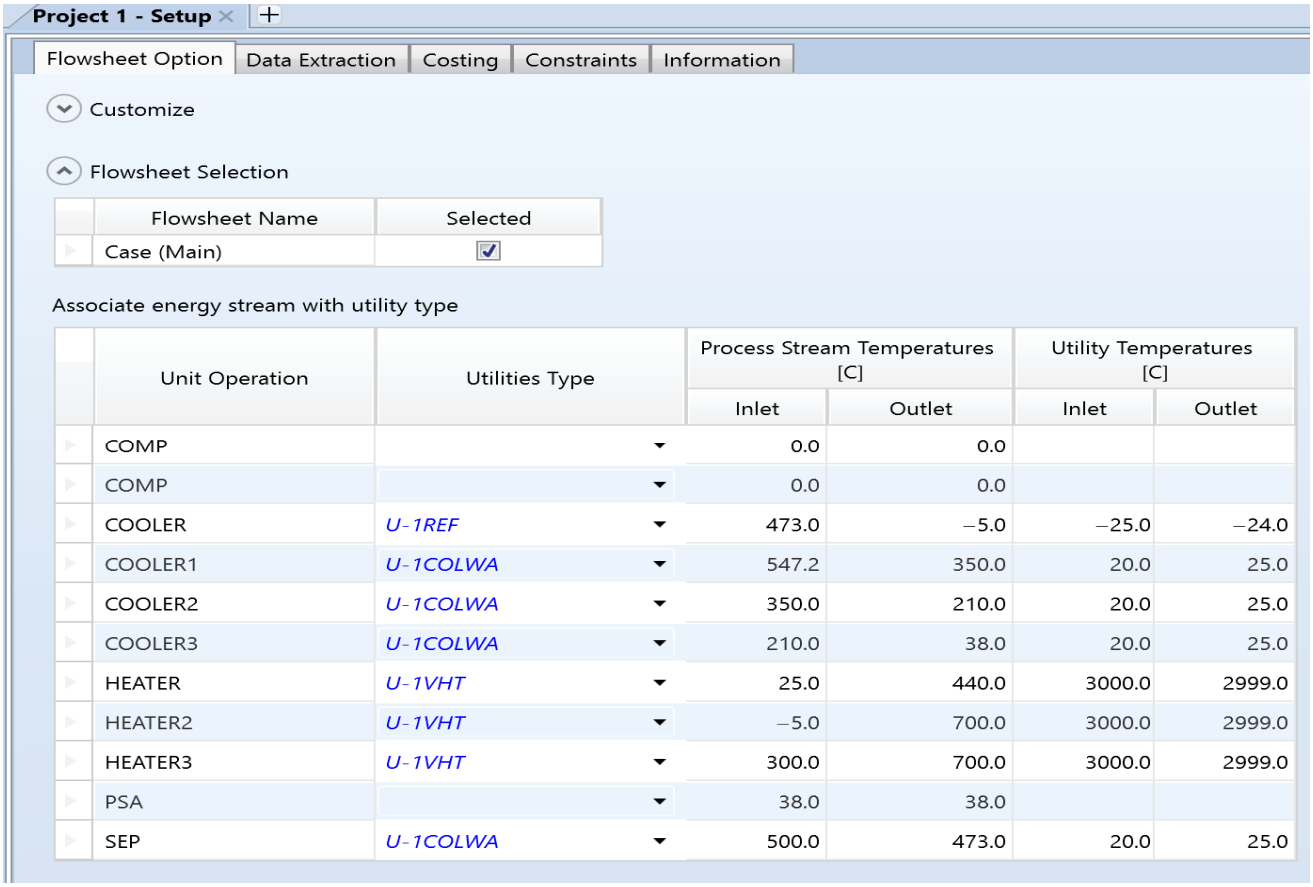

Figure 3. Instruction of allocation required utilities to unit operations.

2.3. Pinch Analysis and Heat Integration

Aspen Plus facilitates preliminary energy analysis through its integration with Aspen Energy Analyser (AEA), a specialised tool for assessing energy-saving potential in chemical processes. AEA enables rapid identification of heat recovery opportunities via pinch point analysis and provides recommendations for improving energy efficiency. While Aspen Plus supports preliminary evaluation, detailed heat integration requires exporting process stream data to AEA, where the heat exchanger network design is performed. AEA is widely used for the design of optimal heat exchanger networks, enabling enhanced heat recovery, reduced utility consumption, and lower operational and environmental costs [102,103]. The tool applies pinch analysis principles to determine optimal utility targets and heat exchange structures between process streams [70].

In this study, Pinch Analysis and heat integration were conducted using Aspen Energy Analyser to minimise reliance on external utilities and reduce the carbon footprint of the production process. Heating and cooling utility demands were systematically evaluated, providing the basis for identifying energy reduction opportunities and for the design of an energy-efficient heat exchanger network. The system boundary for the energy analysis is limited to the on-site process units involved in plastic pyrolysis, reforming, water–gas shift, and hydrogen purification. The analysis considers external utilities required to satisfy heating and cooling demands identified through pinch analysis, and the associated carbon emissions are estimated based on utility sourcing. Upstream processes such as plastic waste collection, sorting, transportation, and preprocessing, as well as capital equipment manufacture and construction, are excluded from the system boundary. Consequently, the results represent process-level energy demand and emissions rather than full lifecycle impacts.

The design of the heat exchanger network was conducted in three primary steps using AEA:

1. Data Extraction: Process simulation data from Aspen Plus, including inlet and outlet temperatures, heat capacities, flow rates, and enthalpy changes, was directly exported to AEA, eliminating manual entry and ensuring accurate input for heat integration analysis Figure 4.
2. Utility Stream Definition: Utilities were defined to supply any additional heating or cooling demands that could not be met by matching hot and cold streams. Appropriate heating and cooling utilities were selected to meet all temperature change requirements for both hot and cold process streams Figure 5.
3. Heat Exchanger Network Design: Using the exported data, AEA generated composite curves for all hot and cold streams, represented as Temperature-Enthalpy (T-Q) diagrams. The pinch point, which separates regions of excess heat (below the pinch) and required heat (above the pinch), was identified to guide the systematic design of an energy-efficient heat exchanger network [76]. A visual representation of the composite curves and the pinch point is shown in Figure 6.

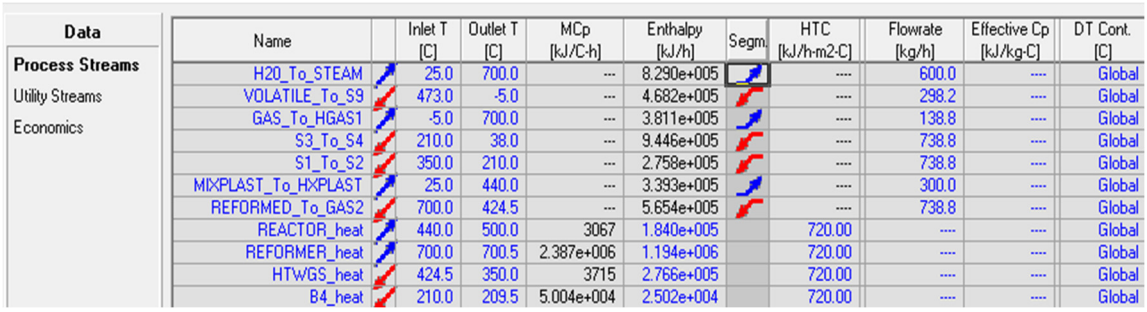

Name	Inlet T [C]	Outlet T [C]	MCp [kJ/C-h]	Enthalpy [kJ/h]	Segm.	HTC [kJ/h-m2-C]	Flowrate [kg/h]	Effective Cp [kJ/kg-C]	DT Cont. [C]
H20_To_STEAM	25.0	700.0	---	8.290e+005		----	600.0	----	Global
VOLATILE_To_S9	473.0	-5.0	---	4.682e+005		----	298.2	----	Global
GAS_To_HGAS1	-5.0	700.0	---	3.811e+005		----	138.8	----	Global
S3_To_S4	210.0	38.0	---	9.446e+005		----	738.8	----	Global
S1_To_S2	350.0	210.0	---	2.758e+005		----	738.8	----	Global
MIXPLAST_To_HXPLAST	25.0	440.0	---	3.393e+005		----	300.0	----	Global
REFORMED_To_GAS2	700.0	424.5	---	5.654e+005		----	738.8	----	Global
REACTOR_heat	440.0	500.0	3067	1.840e+005		720.00	----	----	Global
REFORMER_heat	700.0	700.5	2.387e+006	1.194e+006		720.00	----	----	Global
HTWGS_heat	424.5	350.0	3715	2.766e+005		720.00	----	----	Global
B4_heat	210.0	209.5	5.004e+004	2.502e+004		720.00	----	----	Global

Figure 4. Thermal data extracted from Aspen Plus applied to pinch analysis and heat integration. Red arrows denote hot streams whilst blue arrows denote cold streams.

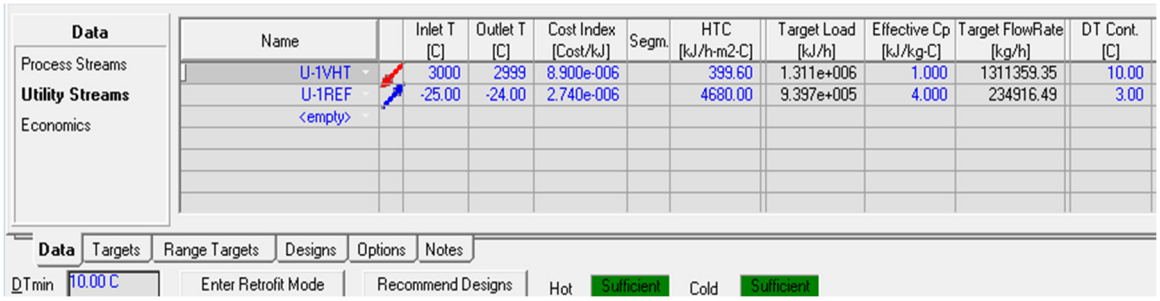

Name	Inlet T [C]	Outlet T [C]	Cost Index [Cost/kJ]	Segm.	HTC [kJ/h-m2-C]	Target Load [kJ/h]	Effective Cp [kJ/kg-C]	Target FlowRate [kg/h]	DT Cont. [C]
U-1VHT	3000	2999	8.900e-006		399.60	1.311e+006	1.000	1311359.35	10.00
U-1REF	-25.00	-24.00	2.740e-006		4680.00	9.397e+005	4.000	234916.49	3.00
<empty>									

Figure 5. Utility stream selection in Aspen Energy Analyser applied to pinch analysis and heat integration. Red arrow denotes hot stream; Blue arrow denotes cold stream.

Principles of Pinch Analysis

To systematically reduce utility consumption and enhance energy efficiency, pinch analysis was applied using composite curves and grid diagrams. Composite curves graphically represent the cumulative heat supply and demand of all hot and cold streams across temperature ranges. The hot composite curve represents the total heat available from hot streams, while the cold composite curve shows the heat required by cold streams. The pinch point, where the curves are closest in temperature, indicates the thermodynamic bottleneck for heat recovery and defines the minimum hot and cold utility requirements [104–106].

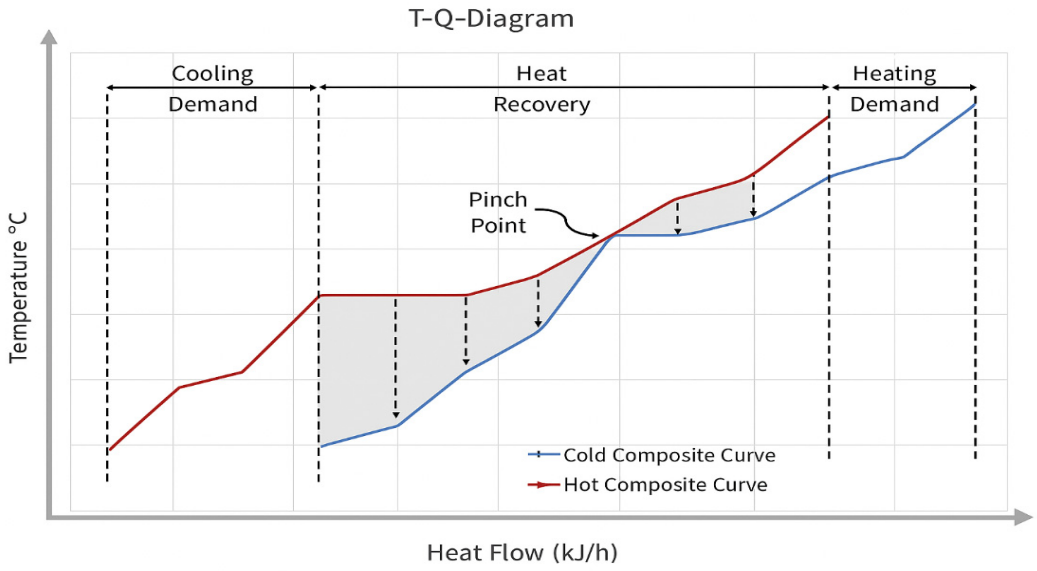

Figure 6. T-Q diagram showing the Hot and Cold composite curve. The arrow shows that heat can be recovered by exchange between the hot and cold streams.

Key principles of pinch analysis were applied to guide the heat exchanger network design:

- No external heating is added below the pinch, and no external cooling is added above the pinch, to prevent increases in overall utility demand.
- Heat transfer across the pinch is avoided to maintain the minimum energy targets.
- Heat exchangers are strategically positioned to maximise energy recovery from process streams while minimising reliance on external utilities.

A grid diagram was used to represent the heat exchanger network, showing hot streams at the top and cold streams at the bottom, with vertical lines connecting streams where heat exchange occurs. The pinch point is indicated to delineate regions of heat surplus and deficit, guiding the placement of exchangers for optimal heat recovery. An example of a Grid diagram for a heat exchanger network is shown in Figure 7. This methodology allows systematic identification of energy-saving opportunities, ensures that the network meets minimum energy targets, and reduces the carbon footprint by minimising external heating and cooling demands.

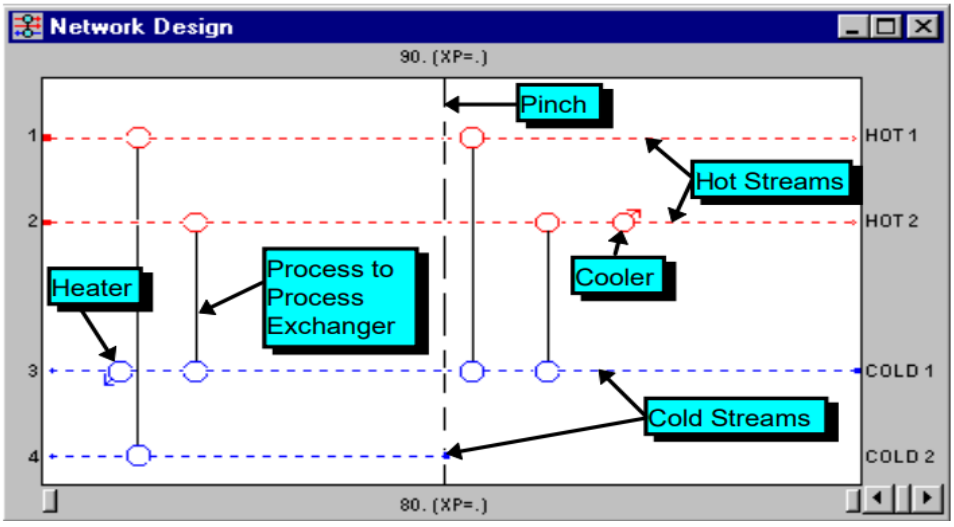

Figure 7. Example of a Grid diagram explaining important parameters in pinch analysis [31].

2.4. Heat Integration Scenarios

Based on this methodology, two optimisation scenarios were evaluated to determine the most techno-economically viable configuration:

Solution 1: Heat integration was implemented by adding heat exchangers to the process to recover heat from process streams. Specifically, a heat exchanger was installed upstream of Cooler 1 on the hot stream and upstream of HEATER3 on the cold stream, enabling heat transfer between process streams rather than relying on external utilities. The resulting modifications to the base-case flowsheet are illustrated in Figure 8.

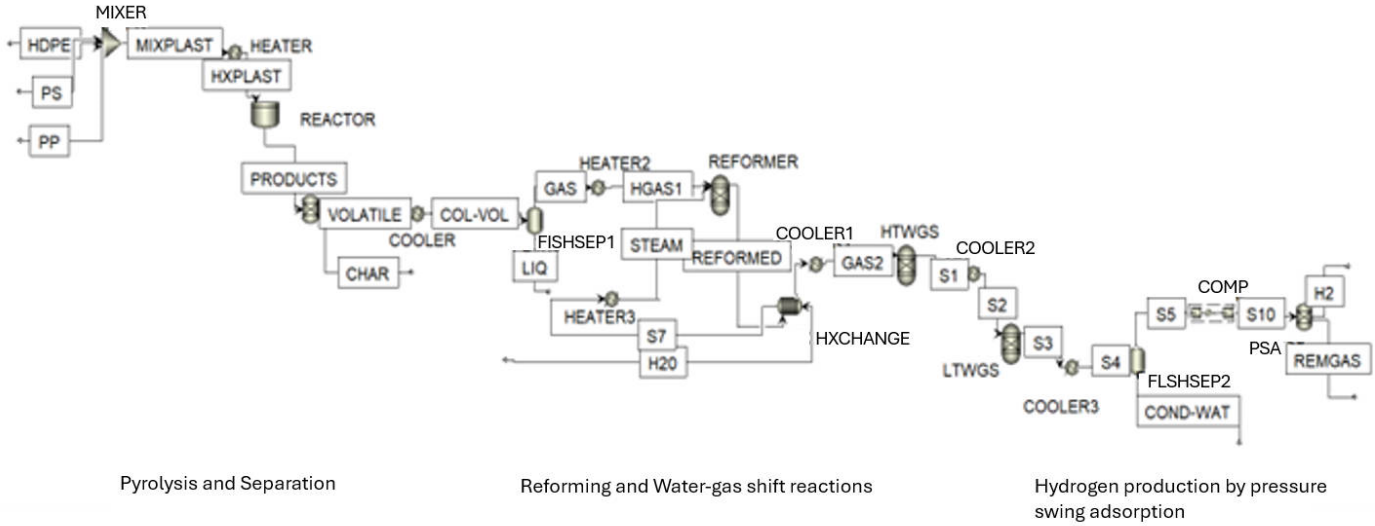

Figure 8. Flowsheet for hydrogen production implementing solution 1 design change. HDPE—High-density polyethylene; PS—Polystyrene; PP—Polypropylene; MIXER—Mixer; MIXPLAST—Plastic mixture; HEATER—Heater for plastic mixture; HXPLAST—Heated plastic mixture; REACTOR—Pyrolysis reactor; PRODUCTS—Product output from pyrolysis reactor; VOLATILE—Volatile stream separated from other pyrolysis product streams; COOLER—Cooler; COL-VOL—Cooled volatile stream; CHAR—Plastic residue; FLSHSEP1—Flash separator to separate gas from liquid; GAS—Gaseous product output from volatile stream; LIQ—Liquid product output stream from volatile stream; HEATER2—Heater for gas; HGAS1—Heated gas stream; REFORMED—Product output from reformer; HEATER3—Heater for steam; S7—Pre-heated steam stream; H2O—Water stream at ambient conditions; HXCHANGE—Heat exchanger; COOLER1—Cooler; GAS2—cooled gas stream; HTWGS—High-temperature water–gas shift reactor; COOLER2—Cooler; LTWGS—Low-temperature water–gas shift reactor; COOLER3—Cooler; S1–S5—Streams 1 to 5 of gas; FLSHSEP2—Flash separator; COND-WAT—Condensed water; COMP—Compressor; S10—Compressed gas; PSA—Pressure swing adsorption column; H2—Hydrogen; REMGAS—Remnant gas (Tail gas).

Solution 2: An additional heat exchanger was installed upstream of the reactor following the implementation of Solution 1. This modification enabled improved heat recovery from the high-enthalpy VOLATILE stream before downstream processing. The resulting configuration represents an advanced heat integration scheme, in which the VOLATILE stream is utilised for multi-stage heat recovery before entering subsequent process units. The corresponding flowsheet modification is shown in Figure 9.

The selection of the optimal configuration was based on energy savings, payback period, additional capital cost, and energy cost savings, while also considering the minimisation of the total number of heat exchange units to ensure industrial feasibility.

The energy-saving potential of the proposed heat integration strategies was quantified using the Available Saving Parameter. This parameter represents the potential reduction in en-

ergy consumption achievable through process optimisation. The Available Savings, expressed as a percentage of the actual energy consumption, were calculated using Equation (1):

$$\text{Available Savings (\% of Actual)} = \left(Q_{Actual} - Q_{Target}/Q_{Actual}\right) \times 100 \quad (1)$$

where the Q_{Actual} values reflect the current energy consumption based on the existing process design, while the Q_{Target} values represent the optimised or theoretical values achievable if all energy-saving opportunities are fully implemented.

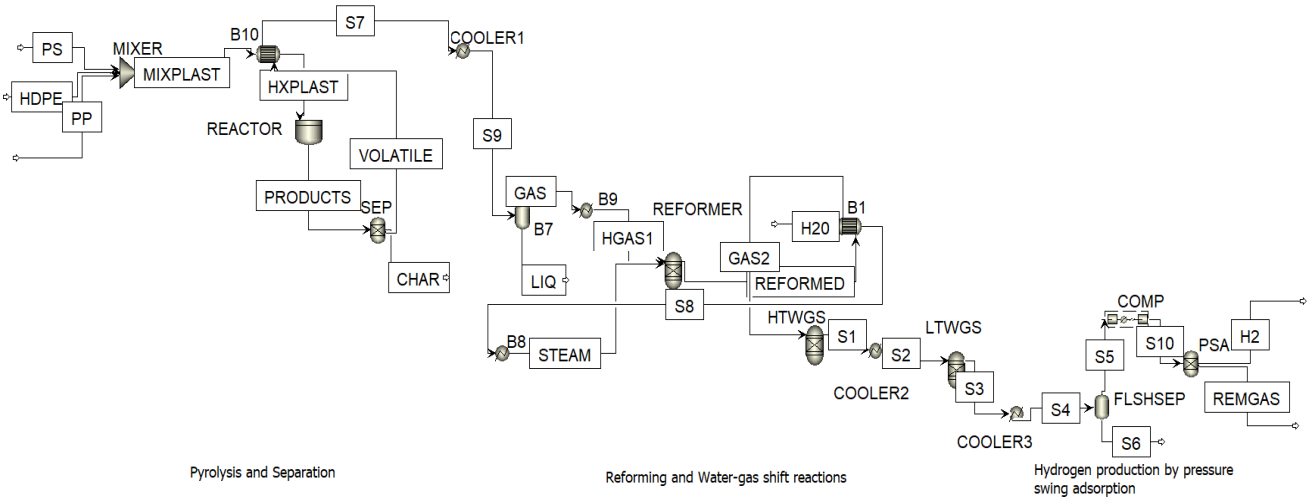

Figure 9. Flowsheet for hydrogen production with heat exchanger integration (solution 2). HDPE—High-density polyethylene; PS—Polystyrene; PP—Polypropylene; MIXER—Mixer; MIXPLAST—Plastic mixture; HEATER—Heater for plastic mixture; HXPLAST—Heated plastic mixture; REACTOR—Pyrolysis reactor; PRODUCTS—Product output from pyrolysis reactor; VOLATILE—Volatile stream separated from other pyrolysis product streams; COOLER—Cooler; SEP—Separator (acting as cyclone); GAS—Gaseous product output from volatile stream; LIQ—Liquid product output stream from volatile stream; B1, B10—Heat exchanger; S1–S10—Streams 1–10; CHAR—Plastic residue stream; COOLER1, COOLER2, COOLER3—Coolers; B8, B9—Heaters; HGAS1—Heated gas stream; REFORMED—Product output from reformer; HTWGS—High-temperature water–gas shift reactor; LTWGS—Low-temperature water–gas shift reactor; FLSHSEP—Flash separator; REM-GAS—Remnant gas; PSA—Pressure swing adsorption; H2—Hydrogen gas.

3. Results and Discussion

3.1. Process Improvement and Energy Savings

The baseline energy analysis of the hydrogen production process identified potential energy savings of 4.27 GJh^{-1}, corresponding to a 59.62% reduction in total utility consumption (Table 1), indicating that instead of the process consuming 100% energy from utilities, only 40.38% would be required, resulting in a 59.62% energy savings. The actual and target energy requirements, including heating and cooling duties, as well as carbon emissions, are summarised in Table 1. The results show that the original process configuration relied heavily on external heating and cooling utilities despite the presence of significant recoverable thermal energy within the system. In particular, the large reduction potential in cooling utilities (85.92%) suggests that a considerable amount of high-temperature heat was being rejected rather than recovered, which is characteristic of thermochemical processes such as pyrolysis and reforming. These findings highlight the inherent inefficiencies of the base case flowsheet when heat recovery is not systematically incorporated during process design.

Table 1. Flow-based summary of energy savings for the base case.

	Actual	Target	Available Savings	% of Actual
Total Utilities (GJh^{-1})	7.14	2.88	1.02	59.62
Heating Utilities (GJh^{-1})	4.67	2.53	0.51	45.65
Cooling Utilities (GJh^{-1})	2.48	0.348	0.51	85.92
Carbon Emissions (kg/h)	206	150.7	55.20	26.80

The reduction in carbon emissions associated with the baseline energy targeting further demonstrates the strong link between thermal inefficiency and environmental performance. Although the base case process was technically feasible, its energy-intensive nature would limit its sustainability if implemented without heat integration, particularly in the context of low-carbon hydrogen production from waste plastics.

Aspen Plus recommended three design modifications to reduce utility consumption, which is shown in Figure 10. Among them, solution 1, which provided the highest energy savings (20.08%) and largest energy cost savings ($41,201/year), was selected for implementation due to its low payback period and minimal extra capital cost. A heat exchanger was added upstream of Cooler 1 for the hot side and upstream of HEATER3 for the cold side, as illustrated in Figure 8. Following this modification, the available energy savings decreased to 2.48 GJh^{-1}, corresponding to a 49.28% reduction in total utilities. These results, which are demonstrated in Table 2, show that incremental design modifications, guided by energy analysis, effectively reduced utility consumption and carbon emissions, confirming the potential of heat integration for improving the energy efficiency of the process.

Figure 10. Design changes recommended by Aspen Plus for process energy enhancement.

Table 2. Flow-based summary of energy savings for the modification recommended by Aspen.

	Actual	Target	Available Savings	% of Actual
Total Utilities (GJh^{-1})	4.98	2.53	0.59	49.28
Heating Utilities (GJh^{-1})	2.82	1.59	0.29	43.49
Cooling Utilities (GJh^{-1})	2.16	0.931	0.29	56.85
Carbon Emissions (kg/h)	189.7	95.13	94.52	49.84

Following the implementation of solution 1, to further improve energy efficiency, an additional heat exchanger was installed before the reactor to recover heat from the volatile stream as shown in Figure 9. This modification optimised heat recovery from the VOLATILE stream. This final modification achieved 1.42 GJh^{-1} savings, corresponding to a 38.72% improvement in energy efficiency compared to the baseline (Table 3).

Table 3. Flow-based summary of energy savings after heat exchanger integration.

	Actual	Target	Available Savings	% of Actual
Total Utilities (GJh^{-1})	3.67	2.25	0.34	38.72
Heating Utilities (GJh^{-1})	2.02	1.31	0.17	35.16
Cooling Utilities (GJh^{-1})	1.65	0.94	0.17	43.08
Carbon Emissions (kg/h)	126.2	79.04	47.14	37.36

This progressive improvement confirms that energy optimisation in complex thermochemical systems is most effective when carried out iteratively. Initial high-impact heat recovery opportunities can be captured through simple modifications, while additional gains require more detailed integration of process streams. The corresponding reduction in carbon emissions across each optimisation stage reinforces the role of heat integration as a dual strategy for both economic and environmental improvement. These results emphasise that systematic energy analysis provides a robust basis for identifying and prioritising design changes in waste-to-hydrogen processes.

3.2. Energy Analysis and Heat Integration

The modified process flowsheet of hydrogen production from plastic wastes (Figure 9) was analysed to evaluate the energy-saving potential through heat integration. Thermal data extracted from the validated Aspen Plus simulation are presented in Figure 4, providing the temperature and enthalpy profiles required for subsequent energy targeting. Based on this thermal information, the appropriate heating and cooling utility streams were selected within Aspen Energy Analyser, as shown in Figure 5.

The composite curves generated from the process thermal data are presented in Figure 11, illustrating the cumulative heat availability of hot streams and the heat demand of cold streams across the operating temperature range. From these curves, the minimum energy targets were identified and are summarised in Figure 12. To illustrate the maximum heat-recovery potential, and in line with standard pinch-analysis practice, the minimum heating and cooling utility requirements were calculated at a ΔTmin of 10 °C. This value represents a technically feasible lower bound commonly used in conceptual pinch analyses for chemical and petrochemical processes. Higher ΔTmin values (e.g., 20–30 °C) would reduce the recoverable heat, but 10 °C provides an upper-bound benchmark for system-level energy evaluation. The resulting heating and cooling utility requirements are 1.311×10^6 kJ/h and 9.397×10^5 kJ/h, respectively. The pinch point was observed at temperatures of approximately 450 °C for the hot streams and 440 °C for the cold streams, indicating the thermodynamic constraint for heat recovery within the process.

The heat exchanger network (HEN) corresponding to the base case configuration without heat integration is shown in Figure 13, with its network performance illustrated in Figure 14. In this configuration, the heating and cooling requirements exceeded the minimum energy targets, operating at 154.2% of the heating target and 175.7% of the cooling target, respectively. This confirms that the initial flowsheet design violated key pinch principles, such as excessive reliance on external utilities and insufficient matching of hot and cold streams near the pinch region.

Following the application of heat integration based on pinch analysis principles, an optimised heat exchanger network was developed, with the position of the heat exchangers within the process flowsheet shown in Figure 9. The corresponding network performance is presented in Figure 15. The optimised network employed three hot utilities, four cold utilities, and thirteen process heat exchangers. As a result, the heating and cooling target percentages were reduced to 106.5% and 111.1%, respectively, indicating a substantial improvement in overall energy efficiency.

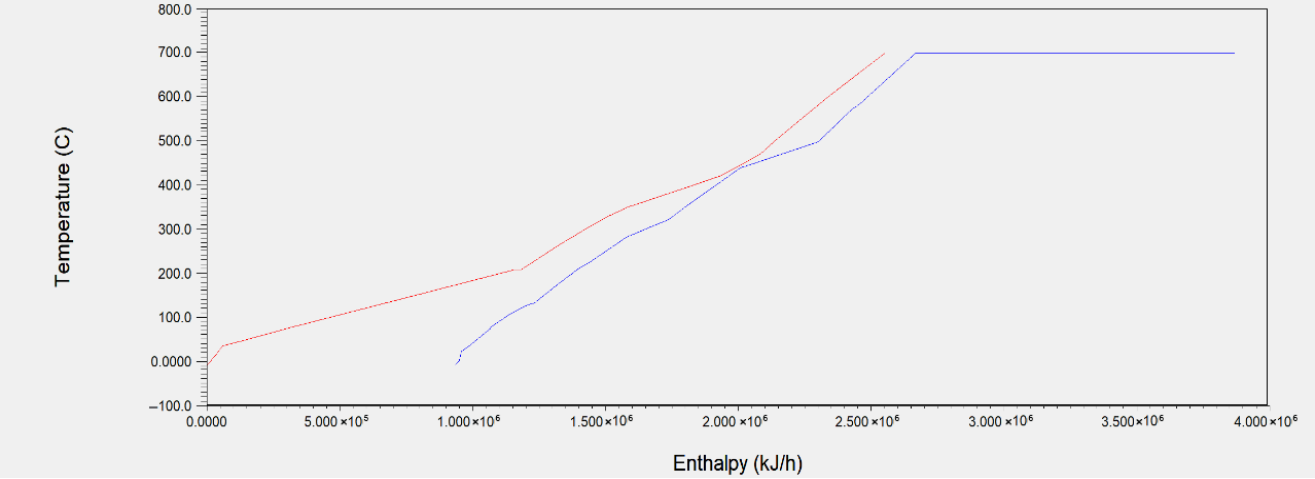

Figure 11. Composite curve for thermal data. Red line represents hot composite curve and blue line represents cold composite curve.

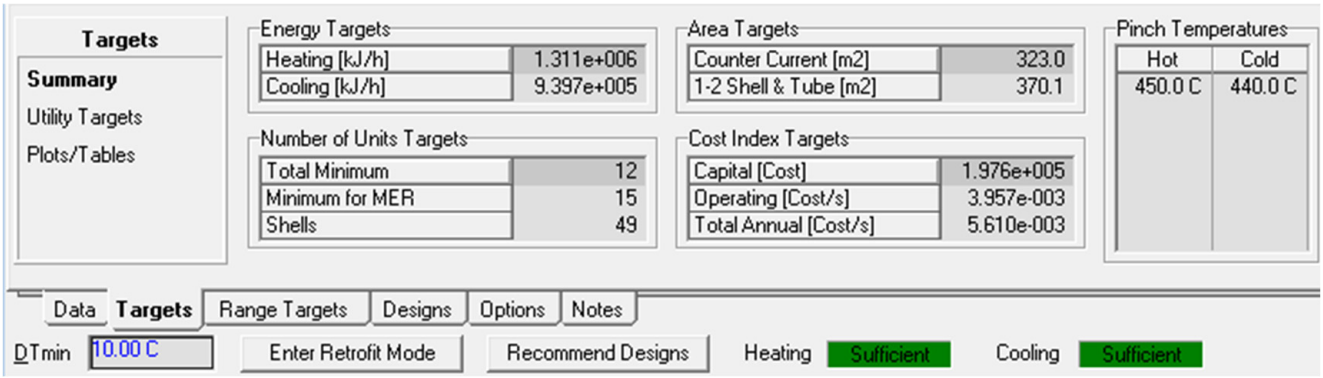

Figure 12. Summary of Energy targets for heating and cooling utility required.

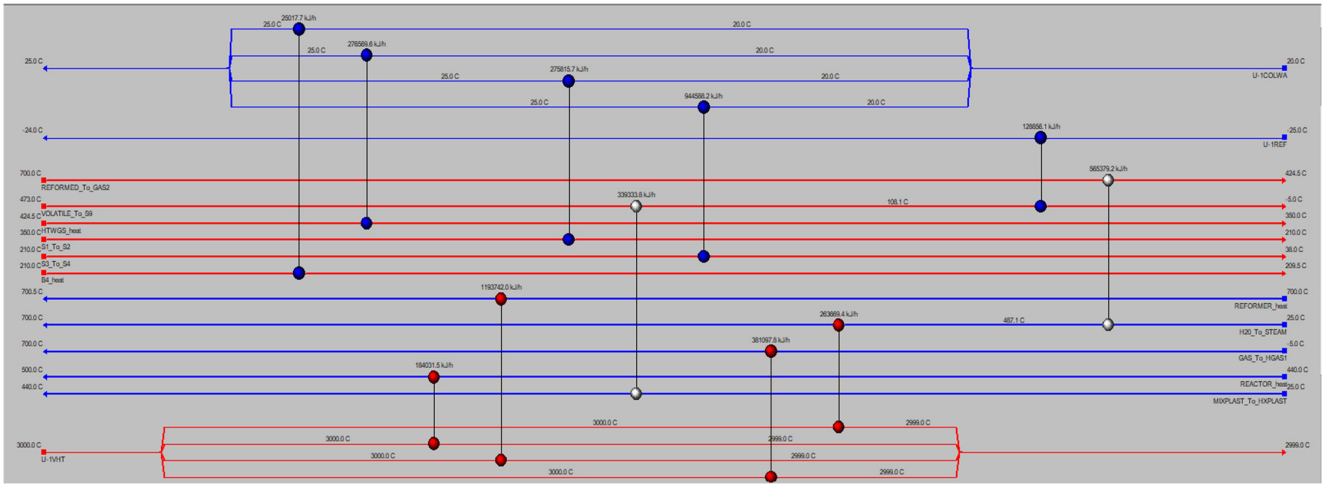

Figure 13. Heat exchanger network of the base case model with no heat integration.

While the minimum targets were not fully reached, the remaining gap can be attributed to practical design constraints, including stream temperature compatibility, ΔT_{min} limitations, and network complexity. Nevertheless, the significant reduction in target exceedance demonstrates the effectiveness of pinch analysis in guiding the development of thermally efficient process designs.

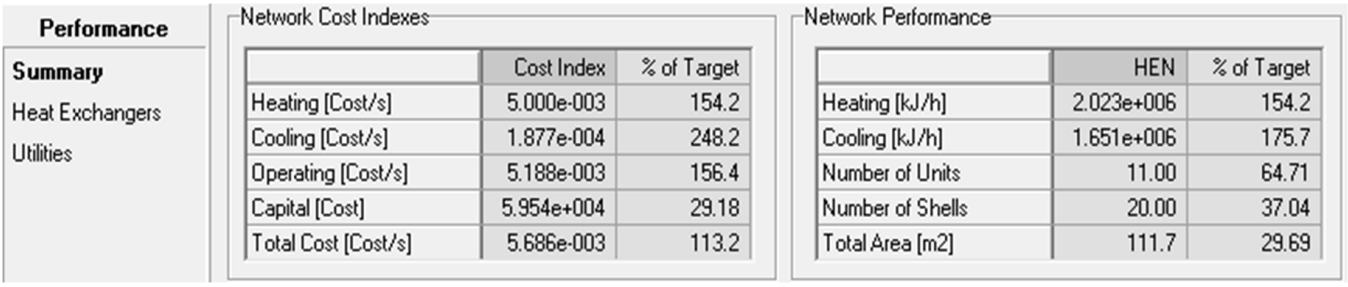

	Cost Index	% of Target
Heating [Cost/s]	5.000e-003	154.2
Cooling [Cost/s]	1.877e-004	248.2
Operating [Cost/s]	5.188e-003	156.4
Capital [Cost]	5.954e+004	29.18
Total Cost [Cost/s]	5.686e-003	113.2

	HEN	% of Target
Heating [kJ/h]	2.023e+006	154.2
Cooling [kJ/h]	1.651e+006	175.7
Number of Units	11.00	64.71
Number of Shells	20.00	37.04
Total Area [m2]	111.7	29.69

Figure 14. Network performance of the base case model without heat integration.

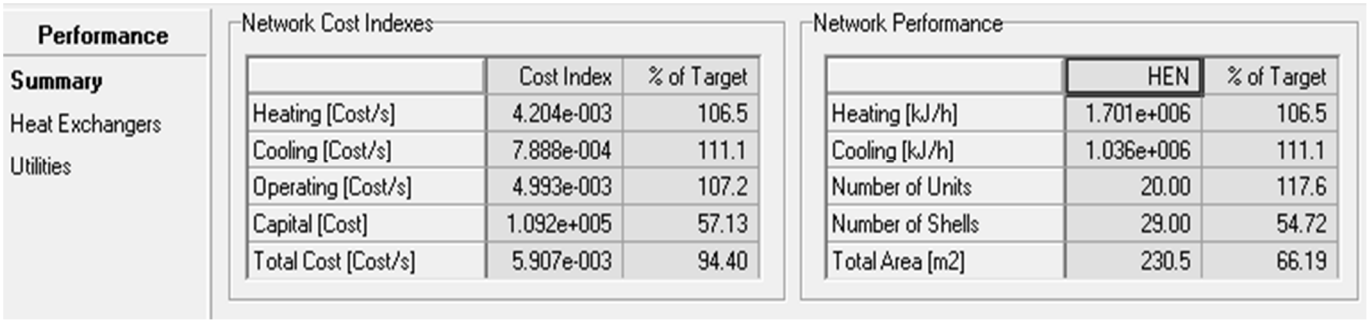

	Cost Index	% of Target
Heating [Cost/s]	4.204e-003	106.5
Cooling [Cost/s]	7.888e-004	111.1
Operating [Cost/s]	4.993e-003	107.2
Capital [Cost]	1.092e+005	57.13
Total Cost [Cost/s]	5.907e-003	94.40

	HEN	% of Target
Heating [kJ/h]	1.701e+006	106.5
Cooling [kJ/h]	1.036e+006	111.1
Number of Units	20.00	117.6
Number of Shells	29.00	54.72
Total Area [m2]	230.5	66.19

Figure 15. Network performance of the heat exchanger network incorporating heat integration.

The heat integration targets identified through pinch analysis represent achievable energy recovery targets that can guide practical industrial design. The heat-exchanger network developed using Aspen Energy Analyzer is based on established pinch-analysis principles and reflects industrially relevant heat-integration strategies commonly applied at the conceptual and preliminary design stages. High-temperature heat exchange is standard practice in thermochemical processes and can be accommodated through appropriate material selection, such as high-temperature alloys, together with staged heat recovery across multiple temperature levels. In addition, temperature control and gas-cleaning steps prior to heat exchange can be implemented to mitigate fouling and deposition risks, which are well-established considerations in industrial heat-exchanger design. These factors guide detailed engineering design prior to implementation. Accordingly, the heat-exchanger network developed in this study is considered industrially feasible, while recognising that final equipment design would be adapted to plant-specific requirements.

4. Conclusions

This study demonstrates that hydrogen production from mixed plastic waste via pyrolysis and in-line reforming can be fundamentally re-positioned from an inherently energy-intensive concept to a thermally efficient and environmentally credible process when systematic energy integration is embedded at the design stage. High operating temperatures, traditionally regarded as a disadvantage of thermochemical waste conversion, are shown here to represent a strategic asset, as they generate substantial opportunities for internal heat recovery. When such opportunities are not deliberately exploited, the process becomes unavoidably dependent on external utilities, eroding both its economic feasibility and its alignment with sustainability objectives.

By integrating rigorous steady-state process modelling with pinch-guided heat integration, this work advances beyond descriptive energy assessment to actively quantify, prioritise, and realise recoverable thermal energy within the system. The baseline analysis revealed that the original flowsheet relied disproportionately on external heating and cooling despite the presence of significant internal heat sources. Application of pinch

analysis reduced total external utility demand from 7.14 to 2.88 GJ h^{-1}, corresponding to a 59.6% reduction, alongside a clear decrease in associated carbon emissions. Achieving this magnitude of utility reduction in a high-temperature hydrogen production process is non-trivial and provides compelling evidence that waste-plastic-to-hydrogen systems need not be utility-dominated when energy integration is treated as a core design requirement.

A central contribution of this study is the demonstration that energy optimisation in complex thermochemical systems is inherently iterative rather than singular. Sequential implementation of heat integration strategies, informed initially by Aspen Plus recommendations and refined through Aspen Energy Analyser, showed that early, low-complexity modifications can unlock a large fraction of available energy savings. Subsequent improvements required increasingly targeted integration of high-enthalpy process streams, illustrating the diminishing-return behaviour typical of advanced energy recovery. This structured progression highlights the value of systematic energy analysis in differentiating high-impact design interventions from marginal refinements, thereby supporting decision-making that is both technically sound and industrially realistic.

The findings further underscore that energy efficiency must be embedded at the earliest stages of process design for emerging waste-to-hydrogen technologies. Delayed or retrofit-based heat integration risks entrenching inefficiencies that are costly or impractical to resolve at later stages of development. In this context, pinch-guided heat integration emerges not as an incremental optimisation tool, but as a decisive enabler for aligning waste-derived hydrogen production with low-carbon energy transition goals.

Overall, this work establishes a robust and transferable framework for evaluating and improving the thermal performance of high-temperature hydrogen production systems based on plastic waste. By explicitly linking process configuration, heat recovery potential, and external utility demand, it delivers design-relevant insights that extend well beyond the specific case examined. The demonstrated reductions in energy consumption and emissions strengthen the case for pyrolysis–reforming pathways as viable components of a circular, low-carbon hydrogen economy, provided that energy integration is recognised and implemented as a foundational design principle rather than a secondary optimisation step.

5. Recommendations for Future Work: System-Level Energy Recovery and Power Integration

While the present study focuses on heat integration through pinch analysis and heat exchanger network optimisation, future work should extend the system boundary to include power-generating energy recovery pathways. In particular, the utilisation of process-derived off-gases for combined heat and power (CHP) generation via gas turbine systems represents a promising direction for enhancing overall process self-sufficiency at scale.

In waste-to-hydrogen systems operating at elevated temperatures, a substantial fraction of the chemical and sensible energy remains embedded in tail gases following hydrogen purification. Converting this energy into electricity and recoverable heat through gas turbine integration could complement conventional heat exchanger-based recovery by addressing energy demands that are not readily met by thermal matching alone. Such an approach would enable a more holistic energy integration strategy, bridging thermal and electrical energy domains within the same process architecture.

However, the integration of gas turbine systems introduces additional design and environmental considerations that warrant further investigation. These include detailed flowsheet development, turbine sizing, part-load performance, dynamic operability, and a rigorous assessment of combustion-related emissions. Importantly, the net environmental benefit of gas turbine integration depends on its interaction with the broader energy system,

including the carbon intensity of displaced grid electricity and the availability of low-carbon utility alternatives.

Future studies should therefore evaluate gas turbine integration in conjunction with carbon capture, utilisation, or storage (CCUS) technologies to mitigate potential emission increases associated with combustion-based energy recovery. For example, by combusting the hydrocarbon-rich gases in a gas turbine or combined heat and power system, overall energy efficiency can be improved. Additionally, integration with carbon capture, utilisation, or storage (CCUS) technologies, such as post-combustion CO_2 capture from flue gas, could further reduce greenhouse gas emissions. The preliminary literature data suggest that hydrocarbon-rich off-gases from plastic pyrolysis can provide sufficient heating value to support small-scale power generation [107–109]. Incorporating these strategies would allow the development of process configurations that maximise energy recovery while minimising environmental impacts. Such coupled assessments would allow the identification of configurations that maximise energy efficiency while maintaining alignment with low-carbon hydrogen objectives. In parallel, techno-economic and policy-oriented analyses should be undertaken to assess carbon credit eligibility, emission penalties, and sensitivity to different utility sourcing scenarios, such as renewable versus fossil-based energy inputs. Additionally, future work could incorporate catalytic kinetic reactor models to assess deviations from equilibrium under industrially relevant operating conditions and to complement the equilibrium-based analysis presented in this study. Benchmarking the pyrolysis–reforming route against alternative hydrogen production pathways, including gasification and electrolysis, would also help contextualise its potential advantages and limitations. Finally, comprehensive environmental assessments, including lifecycle emissions and waste reduction analyses, should be conducted to quantify broader sustainability impacts. Expanding the scope from heat integration alone to integrated heat and power recovery, combined with kinetic modelling, techno-economic evaluation, and environmental assessment, would build upon the foundations of this study and move towards fully optimised, system-level designs for sustainable hydrogen production from plastic waste.

Author Contributions: Conceptualization, K.K.; Methodology, F.J.M., H.R.N. and L.K.; Software, F.J.M. and H.R.N.; Validation, F.J.M., H.R.N. and L.K.; Formal analysis, F.J.M., M.N.G. and L.K.; Investigation, F.J.M., H.R.N., L.K. and K.K.; Resources, H.R.N.; Data curation, F.J.M., M.N.G. and H.R.N.; Writing—original draft, M.N.G.; Writing—review and editing, F.J.M., M.N.G., H.R.N., L.K. and K.K.; Visualization, F.J.M. and H.R.N.; Supervision, H.R.N., L.K. and K.K.; Project administration, H.R.N., L.K. and K.K.; Funding acquisition, H.R.N. All authors have read and agreed to the published version of the manuscript.

Funding: This research received no external funding.

Data Availability Statement: The original contributions presented in this study are included in the article. Further inquiries can be directed to the corresponding author.

Acknowledgments: The author extends sincere gratitude to the Commonwealth Scholarship Commission and the Foreign, Commonwealth, and Development office in the UK for their invaluable support, which made the research presented in this article possible. Gratitude is also extended to the University of Central Lancashire for their collaboration in sponsoring this research.

Conflicts of Interest: The authors declare no conflicts of interest.

References

1. Ghiri, M.N.; Nasriani, H.R.; Khajenoori, L.; Mohammadkhani, S.; Williams, K.S. Dynamic Temperature–Vacuum Swing Adsorption for Sustainable Direct Air Capture: Parametric Optimisation for High-Purity CO_2 Removal. *Sustainability* **2025**, *17*, 6796. [CrossRef]

2. Nasiri-Ghiri, M.; Nasriani, H.R.; Khajenoori, L.; Rasmussen, S.K.; Williams, K. Surrogate-assisted cyclic performance optimisation of direct air capture using amine-functionalised metal–organic frameworks. *Sep. Purif. Technol.* **2025**, *383*, 136177. [CrossRef]
3. Kamara-Esteban, O.; Pijoan, A.; Alonso-Vicario, A.; Borges, C.E. On-demand energy monitoring and response architecture in a ubiquitous world. *Pers. Ubiquitous Comput.* **2017**, *21*, 537–551. [CrossRef]
4. Soroush, M.; Shahbakhti, M. Special issue on "Optimal design and operation of energy systems". *Optim. Control. Appl. Methods* **2023**, *44*, 351–354. [CrossRef]
5. Mohr, T.; Aliyu, H.; Biebinger, L.; Gödert, R.; Hornberger, A.; Cowan, D.; de Maayer, P.; Neumann, A. Effects of different operating parameters on hydrogen production by *Parageobacillus thermoglucosidasius* DSM 6285. *AMB Express* **2019**, *9*, 207. [CrossRef]
6. Lahafdoozian, M.; Khoshkroudmansouri, H.; Zein, S.H.; Jalil, A.A. Hydrogen production from plastic waste: A comprehensive simulation and machine learning study. *Int. J. Hydrogen Energy* **2024**, *59*, 465–479. [CrossRef]
7. Singla, M.K.; Nijhawan, P.; Oberoi, A.S. Hydrogen fuel and fuel cell technology for cleaner future: A review. *Environ. Sci. Pollut. Res.* **2021**, *28*, 15607–15626. [CrossRef]
8. Nasriani, H.R.; Borazjani, A.A.; Iraji, B.; MoradiDowlatAbad, M. Investigation into the effect of capillary number on productivity of a lean gas condensate reservoir. *J. Pet. Sci. Eng.* **2015**, *135*, 384–390. [CrossRef]
9. Nasriani, H.R.; Asadi, E.; Nasiri, M.; Khajenoori, L.; Masihi, M. Challenges of Fluid Phase Behavior Modeling in Iranian Retrograde Gas Condensate Reservoirs. *Energy Sources Part A Recover. Util. Environ. Eff.* **2015**, *37*, 663–669. [CrossRef]
10. Vardian, M.; Nasriani, H.R.; Faghihi, R.; Vardian, A.; Jowkar, S. Porosity and permeability prediction from well logs using an adaptive neuro-fuzzy inference system in a naturally fractured gas-condensate reservoir. *Energy Sources Part A Recover. Util. Environ. Eff.* **2016**, *38*, 435–441. [CrossRef]
11. Nasriani, H.R.; Kalantariasl, A. Choke Performance in High-rate Gas Condensate Wells Under Subcritical Flow Condition. *Energy Sources Part A Recover. Util. Environ. Eff.* **2014**, *37*, 192–199. [CrossRef]
12. Badiei, A.; Jadowski, E.; Sadati, S.; Beizaee, A.; Li, J.; Khajenoori, L.; Nasriani, H.R.; Li, G.; Xiao, X. The Energy-Saving Potential of Air-Side Economisers in Modular Data Centres: Analysis of Opportunities and Risks in Different Climates. *Sustainability* **2023**, *15*, 10777. [CrossRef]
13. Nasriani, H.R.; Jamiolahmady, M. Flowback cleanup mechanisms of post-hydraulic fracturing in unconventional natural gas reservoirs. *J. Nat. Gas Sci. Eng.* **2019**, *66*, 316–342. [CrossRef]
14. Nasriani, H.R.; Jamiolahmady, M. Maximizing fracture productivity in unconventional fields; analysis of post hydraulic fracturing flowback cleanup. *J. Nat. Gas Sci. Eng.* **2018**, *52*, 529–548. [CrossRef]
15. Nasriani, H.R.; Jamiolahmady, M.; Saif, T.; Sánchez, J. A systematic investigation into the flowback cleanup of hydraulic-fractured wells in unconventional gas plays. *Int. J. Coal Geol.* **2018**, *193*, 46–60. [CrossRef]
16. Nasriani, H.R.; Jamiolahmady, M. Permeability Jailbreak: A Deep Simulation Study of Hydraulic Fracture Cleanup in Heterogeneous Tight Gas Reservoirs. *Energies* **2025**, *18*, 3618. [CrossRef]
17. Nasriani, H.R.; Jamiolahmady, M. Optimising Flowback Strategies in Unconventional Reservoirs: The Critical Role of Capillary Forces and Fluid Dynamics. *Energies* **2024**, *17*, 5822. [CrossRef]
18. Joonaki, E.; Rostaminikoo, E.; Ghanaatian, S.; Nasriani, H. Thermodynamics of Hydrogen; Analysing and Refining of Critical Flow Factor Through Comprehensive Uncertainty Assessment and Experimental Data Integration. In Proceedings of the Abu Dhabi International Petroleum Exhibition and Conference, Abu Dhabi, United Arab Emirates, 4–7 November 2024; Paper Number: SPE-222973-MS. [CrossRef]
19. Rehman, A.U.; Sanjari, M.J.; Elavarasan, R.M.; Jamal, T. Sustainability-aligned pathways for energy transition: A review of low-carbon energy network solutions. *Renew. Sustain. Energy Rev.* **2026**, *226*, 116428. [CrossRef]
20. Oyedepo, S.O.; Waheed, M.A.; Abam, F.I.; Dirisu, J.O.; Samuel, O.D.; Ajayi, O.O.; Somorin, T.; Popoola, A.P.I.; Kilanko, O.; Babalola, P.O. A critical review on enhancement and sustainability of energy systems: Perspectives on thermo-economic and thermo-environmental analysis. *Front. Energy Res.* **2025**, *12*, 1417453. [CrossRef]
21. Nabwey, H.A.; Ashraf, M.; Nadeem, H.; Rashad, A.M.; Chamkha, A.J. Optimizing renewable energy systems: A comprehensive review of entropy generation minimization. *AIP Adv.* **2024**, *14*, 120702. [CrossRef]
22. Ukoba, K.; Olatunji, K.O.; Adeoye, E.; Jen, T.-C.; Madyira, D.M. Optimizing renewable energy systems through artificial intelligence: Review and future prospects. *Energy Environ.* **2024**, *35*, 3833–3879. [CrossRef]
23. Mohseni, S.; Brent, A.C. Long-term planning optimisation of sustainable energy systems: A systematic review and meta-analysis of trends, drivers, barriers, and prospects. *Energy Strat. Rev.* **2025**, *57*, 101640. [CrossRef]
24. Klemeš, J.J.; Foley, A.; You, F.; Aviso, K.; Su, R.; Bokhari, A. Sustainable energy integration within the circular economy. *Renew. Sustain. Energy Rev.* **2023**, *177*, 113143. [CrossRef]
25. Akpasi, S.O.; Anekwe, I.M.S.; Tetteh, E.K.; Amune, U.O.; Mustapha, S.I.; Kiambi, S.L. Hydrogen as a clean energy carrier: Advancements, challenges, and its role in a sustainable energy future. *Clean Energy* **2025**, *9*, 52–88. [CrossRef]

26. Segovia-Hernández, J.G.; Hernández, S.; Cossío-Vargas, E.; Juarez-García, M.; Sánchez-Ramírez, E. Green hydrogen production for sustainable development: A critical examination of barriers and strategic opportunities. *RSC Sustain.* **2024**, *3*, 134–157. [CrossRef]
27. de Moraes, D.R.; Soares, L.O.; Guimarães, V.d.A.; Santos, D.C.L.e.P.; Boloy, R.A.M. Technology roadmap of low-carbon hydrogen: Trends for risk management strategies. *Process. Saf. Environ. Prot.* **2025**, *203*, 107937. [CrossRef]
28. Badrudeen, T.U.; David, L.O.; Nwulu, N. Management of environmental and economic tradeoffs for the optimization of renewable energy scheme. *Int. J. Sustain. Energy* **2024**, *43*, 2355645. [CrossRef]
29. Rostaminikoo, E.; Ghanaatian, S.; Joonaki, E.; Nasriani, H.R.; Whitton, J. Advanced thermodynamics of hydrogen and natural gas blends for gas transmission and distribution networks. *Meas. Sens.* **2025**, *38*, 101765. [CrossRef]
30. Joonaki, E.; Rostaminikoo, E.; Ghanaatian, S.; Nasriani, H.R. Thermodynamic properties of hydrogen containing systems and calculation of gas critical flow factor. *Meas. Sens.* **2025**, *38*, 101587. [CrossRef]
31. Gholami, S.; Rostaminikoo, E.; Khajenoori, L.; Nasriani, H.R. Density determination of CO_2-Rich fluids within CCUS processes. *Meas. Sens.* **2025**, *38*, 101739. [CrossRef]
32. Gandomkar, A.; Torabi, F.; Nasriani, H.R.; Enick, R.M. Maximising CO_2 sequestration efficiency in deep saline aquifers through in-situ generation of CO_2-in-brine foam incorporating novel CO_2-soluble non-ionic surfactants. *Chem. Eng. J.* **2025**, *521*, 166102. [CrossRef]
33. Medaiyese, F.J.; Nasriani, H.R.; Khajenoori, L.; Khan, K.; Badiei, A. From Waste to Energy: Enhancing Fuel and Hydrogen Production through Pyrolysis and In-Line Reforming of Plastic Wastes. *Sustainability* **2024**, *16*, 4973. [CrossRef]
34. Jawarneh, A.M.; Al-Oqla, F.M.; Otair, M. Enhancing Photovoltaic Efficiency through Paraffin–Pomegranate Phase Change Composites: An Experimental Approach with Bibliometric Analysis toward Sustainable Thermal Management Aligned with Sustainable Development Goals (SDGs). *ASEAN J. Sci. Eng. Mater.* **2026**, *5*, 249–266.
35. Sang, J.; Zhang, K.; Fan, Q.; Kan, C.; Pan, R.; Sun, X.; Guo, Z. Autophagy–senescence interplay in kidney disease: Mechanistic insights and therapeutic potential. *Mol. Biol. Rep.* **2025**, *53*, 22. [CrossRef]
36. Marefat, A.; Golzary, A.; Bazargan, A.; Nikoo, M.R.; Chihiro, Y. Economic assessment of waste-to-energy technologies for carbon emissions reduction in developing countries: An innovative methodological approach. *Energy Rep.* **2026**, *15*, 108908. [CrossRef]
37. Allan, A.M.; Hasan, A.N.; Shongwe, T. Optimization of waste heat utilization from green hydrogen PEM electrolyzers for enhanced energy efficiency in hot climates: A Persian Gulf region airport study. *Energy Rep.* **2026**, *15*, 108923. [CrossRef]
38. Jain, H.; Dhupper, R. Holistic strategies for sustainable buildings and their impacts on soil and environmental health. *J. Build. Pathol. Rehabil.* **2026**, *11*, 10. [CrossRef]
39. Indonesia, U.; Fitrianto, F.; Putra, N.; Kusrini, E. Review of Sustainable Jet Fuel Production through Pyrolysis of Waste Tires: Process, The Physicochemical Properties and Catalyst. *Kompleks. Ispolz. Miner. Syra* **2026**, *339*, 52–70. [CrossRef]
40. Miwornunyuie, N.; Hunter, J.; Kang, D.; Chavis, C. Advancing biomass-to-energy pathways: Research and development trends in microbial fuel cells for food waste valorization. *Biomass Bioenergy* **2026**, *208*, 108815. [CrossRef]
41. Jakovac, P. The Influence of Energy Trends on the Global Economy. Available online: https://eman-conference.org/wp-content/uploads/2022/12/EMAN_2022_BoA-WEB.pdf#page=106 (accessed on 29 December 2025).
42. Pilapitiya, P.N.T.; Ratnayake, A.S. The world of plastic waste: A review. *Clean. Mater.* **2024**, *11*, 100220. [CrossRef]
43. Dokl, M.; Copot, A.; Krajnc, D.; Van Fan, Y.; Vujanović, A.; Aviso, K.B.; Tan, R.R.; Kravanja, Z.; Čuček, L. Global projections of plastic use, end-of-life fate and potential changes in consumption, reduction, recycling and replacement with bioplastics to 2050. *Sustain. Prod. Consum.* **2024**, *51*, 498–518. [CrossRef]
44. Houssini, K.; Li, J.; Tan, Q. Complexities of the global plastics supply chain revealed in a trade-linked material flow analysis. *Commun. Earth Environ.* **2025**, *6*, 257. [CrossRef]
45. Global Plastic Production | Statista. Available online: https://www.statista.com/statistics/282732/global-production-of-plastics-since-1950/ (accessed on 1 January 2026).
46. Plastics the Fast Facts 2025 • Plastics Europe. Available online: https://plasticseurope.org/knowledge-hub/plastics-the-fast-facts-2025/ (accessed on 1 January 2026).
47. Ladrero, P.B.; Jeffery, L. Regional Priorities For Tackling Plastic Life Cycle Impacts. 2025. Available online: https://newclimate.org/resources/publications/regional-priorities-for-tackling-plastic-lifecycle-impacts (accessed on 1 January 2026).
48. Kan, M.; Wang, C.; Zhu, B.; Chen, W.; Liu, Y.; Ren, Y.; Xu, M. Seven decades of plastic flows and stocks in the United States and pathways toward zero plastic pollution by 2050. *J. Ind. Ecol.* **2023**, *27*, 1538–1552. [CrossRef]
49. Plastics Market Size, Share, Trends | Growth Report [2025–2032]. Available online: https://www.fortunebusinessinsights.com/plastics-market-102176 (accessed on 1 January 2026).
50. Plastic Market Size & Industry Report, 2033. Available online: https://www.marketgrowthreports.com/market-reports/plastic-market-113376 (accessed on 1 January 2026).
51. Plastics Market Size to Hit USD 980.86 Billion by 2034. Available online: https://www.precedenceresearch.com/plastics-market (accessed on 1 January 2026).

52. Ritchie, H.; Samborska, V.; Roser, M. Plastic Pollution. Available online: https://ourworldindata.org/plastic-pollution (accessed on 1 January 2026).
53. Lau, W.W.Y.; Shiran, Y.; Bailey, R.M.; Cook, E.; Stuchtey, M.R.; Koskella, J.; Velis, C.A.; Godfrey, L.; Boucher, J.; Murphy, M.B.; et al. Evaluating scenarios toward zero plastic pollution. *Science* **2020**, *369*, 1455–1461. [CrossRef] [PubMed]
54. Ramaswamy, S.; Kaveri, V.; Sutha, V.; Selvakumar, D.; Geethalakshmi, N.; Mohan, S. The Plastic Trade Web: An In-depth Look at Global Production, Consumption, and Export-Import Trends. *Int. J. Nov. Res. Dev.* **2024**, *9*, 12.
55. Jambeck, J.R.; Geyer, R.; Wilcox, C.; Siegler, T.R.; Perryman, M.; Andrady, A.; Narayan, R.; Law, K.L. Plastic waste inputs from land into the ocean. *Science* **2015**, *347*, 768–771. [CrossRef]
56. Mirkarimi, S.M.R.; Bensaid, S.; Chiaramonti, D. Conversion of mixed waste plastic into fuel for diesel engines through pyrolysis process: A review. *Appl. Energy* **2022**, *327*, 120040. [CrossRef]
57. Barbarias, I.; Lopez, G.; Artetxe, M.; Arregi, A.; Bilbao, J.; Olazar, M. Valorisation of different waste plastics by pyrolysis and in-line catalytic steam reforming for hydrogen production. *Energy Convers. Manag.* **2018**, *156*, 575–584. [CrossRef]
58. Alvarez, J.; Kumagai, S.; Wu, C.; Yoshioka, T.; Bilbao, J.; Olazar, M.; Williams, P.T. Hydrogen production from biomass and plastic mixtures by pyrolysis-gasification. *Int. J. Hydrogen Energy* **2014**, *39*, 10883–10891. [CrossRef]
59. Niu, F.; Wu, Z.; Chen, D.; Huang, Y.; Ordomsky, V.V.; Khodakov, A.Y.; Van Geem, K.M. State-of-the-art and perspectives of hydrogen generation from waste plastics. *Chem. Soc. Rev.* **2025**, *54*, 4948–4972. [CrossRef] [PubMed]
60. Devi, L.; Ptasinski, K.J.; Janssen, F.J. A review of the primary measures for tar elimination in biomass gasification processes. *Biomass Bioenergy* **2003**, *24*, 125–140. [CrossRef]
61. Shah, H.H.; Amin, M.; Iqbal, A.; Nadeem, I.; Kalin, M.; Soomar, A.M.; Galal, A.M. A review on gasification and pyrolysis of waste plastics. *Front. Chem.* **2023**, *10*, 960894. [CrossRef]
62. Han, D.; Shin, S.; Jung, H.; Cho, W.; Baek, Y. Hydrogen Production by Steam Reforming of Pyrolysis Oil from Waste Plastic over 3 wt.% Ni/Ce-Zr-Mg/Al_2O_3 Catalyst. *Energies* **2023**, *16*, 2656. [CrossRef]
63. Alshareef, R.; Nahil, M.A.; Williams, P.T. Hydrogen production by three-stage (i) pyrolysis,(ii) catalytic steam reforming, and (iii) water gas shift processing of waste plastic. *Energy Fuels* **2023**, *37*, 3894–3907. [CrossRef] [PubMed]
64. Pawelczyk, E.; Wysocka, I.; Gębicki, J. Pyrolysis combined with the dry reforming of waste plastics as a potential method for resource recovery—A review of process parameters and catalysts. *Catalysts* **2022**, *12*, 362. [CrossRef]
65. Sudalaimuthu, P.; Sathyamurthy, R. The clean energy aspect of plastic waste—Hydrogen gas production, CO_2 reforming, and plastic waste management coincide with catalytic pyrolysis—An extensive review. *Environ. Sci. Pollut. Res.* **2023**, *30*, 66559–66584. [CrossRef]
66. Soleimani, S.; Lehner, M. Tri-reforming of methane: Thermodynamics, operating conditions, reactor technology and efficiency evaluation—A review. *Energies* **2022**, *15*, 7159. [CrossRef]
67. Uddin, M.; Rasul, M.; Chowdhury, A.A.; Hassan, N. Hydrogen production from plastic waste pyrolysis syngas: A review on progresses and challenges. *Int. J. Hydrogen Energy* **2025**, *158*, 150512. [CrossRef]
68. Ren, Z.; Gao, Z.; Guo, Z.; Liu, P.; Yao, D. Sustainable hydrogen production from waste plastics via staged chemical looping gasification with iron-based oxygen carrier. *Appl. Energy Combust. Sci.* **2025**, *23*, 100362. [CrossRef]
69. Boshagh, F.; Yoon, H.-J.; Lee, C.-J. Key parameters influencing steam-reforming performance for hydrogen production. *Renew. Sustain. Energy Rev.* **2025**, *218*, 115777. [CrossRef]
70. Haydary, J. Energy Integration. In *Chemical Process Design and Simulation*; John Wiley & Sons, Inc.: Hoboken, NJ, USA, 2018; pp. 239–261. [CrossRef]
71. Heat Exchanger Network Analysis of the Power Plant Industry Using Aspen Energy Analyzer Software—Institut Teknologi Sepuluh Nopember (ITS), Indonesia. Available online: https://scholar.its.ac.id/en/publications/heat-exchanger-network-analysis-of-the-power-plant-industry-using/ (accessed on 29 December 2025).
72. Gollangi, R.; NagamalleswaraRao, K. Energy, exergy analysis of conceptually designed monochloromethane production process from hydrochlorination of methanol. *Energy* **2022**, *239*, 121858. [CrossRef]
73. Abdul, A.Z.; Ngulde, A.B.; Khan, G.; Abubakar, A.M.; Abass, A. Energy Analysis of an Existing CO_2 Plant Simulated in Aspen Plus V8.8. *Asian J. Eng. Soc. Health* **2023**, *2*, 1396–1405. [CrossRef]
74. Cortazar, M.; Gao, N.; Quan, C.; Suarez, M.A.; Lopez, G.; Orozco, S.; Santamaria, L.; Amutio, M.; Olazar, M. Analysis of hydrogen production potential from waste plastics by pyrolysis and in line oxidative steam reforming. *Fuel Process. Technol.* **2022**, *225*, 107044. [CrossRef]
75. Williams, P.T. Hydrogen and carbon nanotubes from pyrolysis-catalysis of waste plastics: A review. *Waste Biomass-Valorization* **2020**, *12*, 1–28. [CrossRef]
76. Zoughaib, A. *From Pinch Methodology to Pinch-Exergy Integration of Flexible Systems*; Elsevier: Amsterdam, The Netherlands, 2017.
77. Oh, T.; Lee, S. Optimization of steam-methane reforming process using PSA off gas. *Int. J. Hydrogen Energy* **2024**, *95*, 902–915. [CrossRef]

78. Sun, M.; Duan, L.; Zhou, Y.; Zhang, H.; Huang, L.; Zheng, N. Study on a novel hydrogen purification approach base on methane steam reforming process with CO-preferential oxidation and CO_2 removal. *Appl. Energy* **2025**, *377*, 124727. [CrossRef]
79. Davies, W.G.; Babamohammadi, S.; Yan, Y.; Clough, P.T.; Soltani, S.M. Exergy analysis in intensification of sorption-enhanced steam methane reforming for clean hydrogen production: Comparative study and efficiency optimisation. *Carbon Capture Sci. Technol.* **2024**, *12*, 100202. [CrossRef]
80. Martínez-Rodríguez, A.; Abánades, A. Comparative Analysis of Energy and Exergy Performance of Hydrogen Production Methods. *Entropy* **2020**, *22*, 1286. [CrossRef]
81. Franchi, G.; Capocelli, M.; De Falco, M.; Piemonte, V.; Barba, D. Hydrogen Production via Steam Reforming: A Critical Analysis of MR and RMM Technologies. *Membranes* **2020**, *10*, 10. [CrossRef]
82. Szablowski, L.; Wojcik, M.; Dybinski, O. Review of steam methane reforming as a method of hydrogen production. *Energy* **2025**, *316*, 134540. [CrossRef]
83. Song, C.; Liu, Q.; Ji, N.; Kansha, Y.; Tsutsumi, A. Optimization of steam methane reforming coupled with pressure swing adsorption hydrogen production process by heat integration. *Appl. Energy* **2015**, *154*, 392–401. [CrossRef]
84. Berstad, D.; Gundersen, T. On the exergy efficiency of CO_2 capture: The relation between sub-process and overall efficiencies. *Carbon Capture Sci. Technol.* **2023**, *7*, 100111. [CrossRef]
85. Bahzad, H.; Leonzio, G.; Soltani, S.M.; Al Jasmi, A.; Davies, W.G.; Fennell, P.S.; Ali, N. Techno-economic analyses of a novel hydrogen production process via chemical looping water splitting, integrated with sorption enhanced water gas shift. *Int. J. Hydrogen Energy* **2025**, *188*, 151996. [CrossRef]
86. Escribà-Gelonch, M.; Osorio-Tejada, J.; Yu, L.; Wanten, B.; Bogaerts, A.; Hessel, V. Techno-economic and life-cycle assessment for syngas production using sustainable plasma-assisted methane reforming technologies. *Energy Environ. Sci.* **2025**, *18*, 6043–6062. [CrossRef]
87. Li, Y.; Nahil, M.A.; Williams, P.T. Hydrogen/Syngas Production from Different Types of Waste Plastics Using a Sacrificial Tire Char Catalyst via Pyrolysis–Catalytic Steam Reforming. *Energy Fuels* **2023**, *37*, 6661–6673. [CrossRef]
88. Mishra, R.; Shu, C.; Gollakota, A.; Pan, S. Unveiling the potential of pyrolysis-gasification for hydrogen-rich syngas production from biomass and plastic waste. *Energy Convers. Manag.* **2024**, *321*, 118997. [CrossRef]
89. Amlogu, T.O.; Dayo-Odukoya, O.P. Heat Integration Of Hydrogen Production From Glycerol Reforming. *Int. J. Adv. Res.* **2019**, *7*, 506–518. [CrossRef] [PubMed]
90. Venkatesh, G. Pinch analysis, as a technique for optimising resource utilisation and promoting environmental sustainability: A review of recent case studies from the developing world and transition economies. *Resour. Environ. Inf. Eng.* **2019**, *1*, 1–17. [CrossRef]
91. López-Fernández, A.; Bolonio, D.; Amez, I.; Castells, B.; Ortega, M.F.; García-Martínez, M.-J. Design and Pinch Analysis of a GFT Process for Production of Biojet Fuel from Biomass and Plastics. *Energies* **2021**, *14*, 6035. [CrossRef]
92. Koike, M.; Li, D.; Watanabe, H.; Nakagawa, Y.; Tomishige, K. Comparative study on steam reforming of model aromatic compounds of biomass tar over Ni and Ni–Fe alloy nanoparticles. *Appl. Catal. A Gen.* **2015**, *506*, 151–162. [CrossRef]
93. Medaiyese, F.J.; Nasriani, H.R.; Khan, K.; Khajenoori, L. Sustainable Hydrogen Production from Plastic Waste: Optimizing Pyrolysis for a Circular Economy. *Hydrogen* **2025**, *6*, 15. [CrossRef]
94. Safarian, S.; Rydén, M.; Janssen, M. Development and Comparison of Thermodynamic Equilibrium and Kinetic Approaches for Biomass Pyrolysis Modeling. *Energies* **2022**, *15*, 3999. [CrossRef]
95. Kouas, M.; Torrijos, M.; Sousbie, P.; Harmand, J.; Sayadi, S. Modeling the anaerobic co-digestion of solid waste: From batch to semi-continuous simulation. *Bioresour. Technol.* **2019**, *274*, 33–42. [CrossRef]
96. Insel, G.; Ozyildiz, G.; Okutman-Tas, D.; Guven, D.; Zengin, G.E.; Pala-Ozkok, I.; Kurt, E.S.; Atli, E.; Artan, N.; Takács, I.; et al. A comprehensive evaluation of process kinetics: A plant-wide approach for nutrient removal and biogas production. *Water Res.* **2022**, *217*, 118410. [CrossRef] [PubMed]
97. Levine, S.E.; Broadbelt, L.J. Detailed mechanistic modeling of high-density polyethylene pyrolysis: Low molecular weight product evolution. *Polym. Degrad. Stab.* **2009**, *94*, 810–822. [CrossRef]
98. Kruse, T.M.; Wong, H.-W.; Broadbelt, L.J. Mechanistic modeling of polymer pyrolysis: Polypropylene. *Macromolecules* **2003**, *36*, 9594–9607. [CrossRef]
99. Kruse, T.M.; Woo, O.S.; Wong, H.-W.; Khan, S.S.; Broadbelt, L.J. Mechanistic Modeling of Polymer Degradation: A Comprehensive Study of Polystyrene. *Macromolecules* **2002**, *35*, 7830–7844. [CrossRef]
100. Cirillo, D.; Di Palma, M.; La Villetta, M.; Macaluso, A.; Mauro, A.; Vanoli, L. A novel biomass gasification micro-cogeneration plant: Experimental and numerical analysis. *Energy Convers. Manag.* **2021**, *243*, 114349. [CrossRef]
101. Miranda, R.; Yang, J.; Roy, C.; Vasile, C. Vacuum pyrolysis of commingled plastics containing PVC I. Kinetic study. *Polym. Degrad. Stab.* **2001**, *72*, 469–491. [CrossRef]
102. Aas, E. *Optimization of Heat Exchanger Networks Using Aspen Energy Analyzer and SeqHENS*; Norwegian University of Science and Technology: Trondheim, Norway, 2019.

103. Muharja, M.; Widjaja, A.; Darmayanti, R.F.; Airlangga, B.; Anugraha, R.P.; Fauziyah, M.; Wijanarto, E.; Sholehuddin, M.; Khamil, A.I. Heat Exchanger Network (HEN) Analysis of The Power Plant Industry Using Aspen Energy Analyzer Software. *ASEAN J. Chem. Eng.* **2023**, *23*, 14–27. [CrossRef]
104. Linnhoff, M. Introduction to Pinch Technology. 1998. Available online: https://scholar.google.com/scholar?hl=en&as_sdt=0,5&q=31.%09Linnhoff,+M.+(1998).+Introduction+to+Pinch+Technology.+Targeting+House.&btnG= (accessed on 29 December 2025).
105. Aghahosseini, S.; Dincer, I. Exergy-Based Design and Analysis of Heat Exchanger Networks. In *Progress in Clean Energy, Volume 1: Analysis and Modeling*; Springer: Cham, Switzerland, 2015; pp. 371–387. [CrossRef]
106. Pethe, K.R.; Dabhade, P.M.; Kolekar, V.J.; Sardare, M.D. Heat integration and heat exchanger network design with aspen energy analyze. In *IOP Conference Series: Materials Science and Engineering*; IOP Publishing: Bristol, UK, 2022; Volume 1259, p. 012006. [CrossRef]
107. Kabeyi, M.J.B.; Olanrewaju, O.A. Review and Design Overview of Plastic Waste-to-Pyrolysis Oil Conversion with Implications on the Energy Transition. *J. Energy* **2023**, *2023*, 1821129. [CrossRef]
108. Moliner, C.; Pasquale, G.; Arato, E. Municipal Plastic Waste Recycling through Pyrogasification. *Energies* **2024**, *17*, 1206. [CrossRef]
109. Akinbomi, J.G.; Oresajo, C.A.; Ogunjobi, M.O.; Omotayo, M.S.; Aminu, K.A.; Abdulkareem, Y.T.; Bakare, L. Electricity generation potential of synthetic human hair, water nylon sachet and plastic waste mixtures. *Int. J. Front. Eng. Technol. Res.* **2025**, *8*, 13–18. [CrossRef]